Analytica Chimica Acta 1174 (2021) 338709

Contents lists available at ScienceDirect

Analytica Chimica Acta

journal homepage: www.elsevier.com/locate/aca

An ultra-red fluorescent biosensor for highly sensitive and rapid detection of biliverdin

Xiaqing Zhu [a], Shuren Feng [c], Zhongyi Jiang [d], Huayue Zhang [a], Yanyan Wang [a, **], Haitao Yang [a, b], Zefang Wang [a, b, *]

[a] School of Life Sciences, Tianjin Key Laboratory of Function and Application of Biological Macromolecular Structures, College of Precision Instrument and Opto-electronics Engineering, Tianjin University, Tianjin, 300072, China
[b] Tianjin International Joint Academy of Biotechnology and Medicine, Tianjin, 300457, China
[c] Tianjin Women's and Children's Health Centre (TWCHC), Tianjin, 300051, China
[d] Cleveland Clinic Lerner Research Institute, Cleveland, OH 44195, USA

HIGHLIGHTS

- A novel ultra-red fluorescent protein smURFP was used as a BV-sensing element.
- Detecting condition was systematically optimized base on structural information.
- Physical conditions such as pH and salt concentration can regulate the attachment.
- The LOD of our biosensor (0.4 nM in serum) was the lowest one reported thus far.

GRAPHICAL ABSTRACT

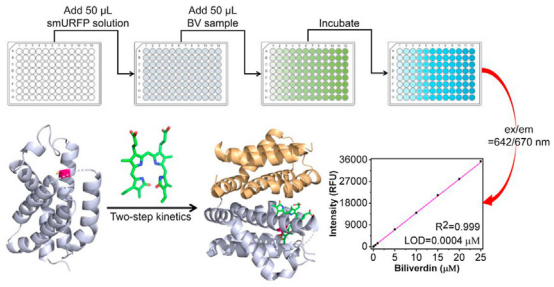

ARTICLE INFO

Article history:
Received 1 January 2021
Received in revised form
20 May 2021
Accepted 27 May 2021
Available online 31 May 2021

Keywords:
Biliverdin
smURFP
Infrared fluorescent protein
Biosensor

ABSTRACT

The important role of BV in clinical diagnostics of liver-related diseases has been established in veterinary medicine. However, the sensitivity and selectivity of the current BV assays remain relatively low compromising its wider application in clinical diagnosis. Herein, we developed a rapid and sensitive BV-detecting biosensor based on a novel far-red fluorescent protein smURFP, which produced fluorescence only through specific interaction with its cofactor BV. In our study, the binding of BV to smURFP was then systematically optimized based on the structures of the smURFP + BV complex to increase the sensitivity of our biosensor. A wide linear range from 0 μM to 25 μM was obtained in both chicken and human serum. The limit of detection (LOD) and limit of quantification (LOQ) for BV was as low as 0.4 nM and 1.5 nM in human serum, and 0.4 nM and 1.2 nM in chicken serum. To our knowledge, this is the lowest LOD that has ever been reported for a BV biosensor. Our study sheds light on the biological and clinical analysis of BV.

* Corresponding author. School of Life Sciences, Tianjin Key Laboratory of Function and Application of Biological Macromolecular Structures, College of Precision Instrument and Opto-electronics Engineering, Tianjin University, Tianjin, 300072, China.
** Corresponding author. Weijin Road Campus of Tianjin University, Tianjin, 300072, China.
E-mail addresses: yanyanwang@tju.edu.cn (Y. Wang), zefangwang@tju.edu.cn (Z. Wang).

https://doi.org/10.1016/j.aca.2021.338709
0003-2670/

1. Introduction

Biliverdin (BV) is a natural green-colored bile pigment. In the spleen, BV is produced by heme oxygenase (HO) opens the tetrapyrrole ring of heme from senescent erythrocytes, which is rapidly converted to bilirubin (BR) by biliverdin reductase (BVR) [1]. Although BV was initially regarded as a catabolite, several studies have proposed its useful effects such as cytoprotective [2,3], anti-inflammatory [3,4], and anti-oxidative effects [5,6]. Also, BV has also been suggested to function as an HIV-1 protease inhibitor [7,8]. Pre-clinical researches have already been done by *in vivo* administration of BV for explaining its beneficial effects in physianthropy such as the regulatory role of BV in transplantation, endotoxemia, vascular injury, and inflammatory disorder models [6,9,10]. Recently, two groups proved that BV could even work as an inherent photoacoustic imaging probe for cancer imaging *in vivo* by using its near-infrared adsorbing property [11,12]. Moreover, in veterinary medicine, it has been suggested that increased concentration of BV in serum indicates anemia caused by intoxication, infection, liver problems or biliary obstruction in birds and reptiles [13,14]. High exposure to toxic compounds producing hemolytic anemia in birds, such as lead, can be manifested by gall-bladder enlargement, viscous bile and green-stained feces [15]. Biliverdinuria is the sign of hepatic disease which occurs as the result of a serum accumulation of BV that exceeds the renal threshold in veterinary practice. Besides, BV is an important avian eggshell pigment which gives the eggshell a blue-green hue, which possesses important physiological properties [16]. Blue eggshell coloration in species with biparental care may function as a post-mating sexual signal of female quality to their mates [17], also may indicate female immunocompetence and condition [18]. Although standard BV test have been established in veterinary medicine as birds and reptiles have little biliverdin reductase activity, it has not been included in standard diagnostic testing in physianthropy. However, studies using BV as a natural substance in clinical diagnosis and treatment indeed have increased the demand for fast and accurate quantification of BV in human biological samples.

High-performance liquid chromatography is the most commonly used one for direct detection of BV molecules in samples [19,20]. Mass spectrometry and fiber enhanced resonance Raman spectroscopy have also been developed based on the fundamental physical properties of BV [21,22]. However, these traditional direct methods have often been criticized due to their high cost, cumbersome operation, and requirement of skilled individuals. In recent years, some indirect methods for BV detection have been developed to overcome the issues related with direct methods. They are based on using sensory elements that can recognize and interact with BV and then produce detectable signals. Sanu et al. reported a fluorescent probe based on an L-cysteine modulated copper nanoclusters for the determination of BV [23]. Novotna et al. applied liposomes and micelles as sensory elements to build a chiroptical method for the analysis of BV [24]. Although the aftermentioned indirect methods can be operated in simple, economical and rapid ways, the sensitivity and selectivity of these methods remain relatively low. Therefore, it is crucial to develop an indirect method with high sensitivity and selectivity.

In this study, we developed a simple and fast fluorescent biosensor foe BV detection using smURFP that was a novel near-infrared fluorescent protein developed in the laboratory of Roger Y. Tsien [25]. smURFP requires BV binding and covalent attachment to produce fluorescence. Therefore, it was an ideal target to test our strategy. We systematically optimized the interaction between BV and smURFP based in the recently reported crystal structure of BV and smURFP [26]. Finally, we obtained a limit of detection (LOD) for BV was as low as 0.4 nM in both human and chicken serum. To the best of our knowledge, this is the lowest LOD that has ever been reported for the BV sensor. We also obtained a wide linear range from 0 μM to 25 μM which is among the best obtained for the thrombin assay as well.

2. Experimental procedures

2.1. Expression and purification of smURFP protein

Coding sequences for smURFP were codon-optimized and synthesized from GENEWIZ (Tianjin, CHINA). The plasmid pET-28b (+)-SUMO-*smurfp* was transformed into *E. coli* BL21 (DE3) strain. The strains were grown in LB broth containing 100 μg mL^{-1} kanamycin at 37 °C, 220 rpm to an OD_{600} of ~0.6. Protein expression was then induced by adding 0.5 mM IPTG and further cultured at 16 °C, 220 rpm for 16 h. The cells were harvested and followed by high pressure cell disruption. Cell lysate was then collected using centrifugation (18,000 rpm, 45 min, 4 °C). Ni-NTA affinity resin (GE Healthcare, USA) was used to capture the 6*His- &SUMO-tagged target proteins in lysate and SUMO tag were removed through on-column cleavage using SUMO protease (ULP) at 4 °C for 18 h. The resulting protein of interest was then applied to a HiTrap™ Q 5 mL column (GE Healthcare, USA) in a linear gradient from 0 mM to 1000 mM NaCl with 50 mM Tris-HCl (pH 8.0). The target protein was collected and further purified using a Superdex 75 10/300 GL column (GE Healthcare, USA) in a buffer consisting of 150 mM NaCl. The purified smURFP was identified by 15% SDS-PAGE.

2.2. Preparation of the BV solutions and other chemicals

BV (Sigma-Aldrich, USA) stock solution (100 mM) was prepared in dimethyl sulfoxide (DMSO). The stock solution was further diluted to 10 mM in different buffers to prepare other BV solutions and stored at −20 °C. BV solution (10 mM) was further diluted in optimal buffer, human serum (Hongquan Bio, CHINA), or chicken serum (Bossbio, CHINA) to prepare the rest of the BV solutions, which were aliquoted. Hematin (BBI Life Sciences, CHINA) was prepared at 10 mM and bilirubin (Frontier Scientific, USA) at 10 mM in DMSO. $BVMe_2$ (Sants Cruz Biotechnology, USA) was prepared at 10 mM in DMSO. Appropriate dilutions of each were made in human serum, chicken serum, or the optimal buffer.

2.3. Measuring the fluorescence of smURFP + BV

50 μL of the purified smURFP solution that had been thawed on ice and centrifuged at 12,000 rpm for 10 min at 4 °C was placed into black 96-well plates, followed by 50 μL of BV sample and mixed by pipetting. Fluorescence (excitation: 642 nm; emission: 670 nm) was measured after incubation at 4 °C in the dark using the PerkinElimer EnSpire® multimode plate reader with the Z-position set at 18,500 μm, gain set at optimal, and 8 reads per well. All samples were assayed in duplicate.

2.4. Optimization of the binding of BV to smURFP

The effects of pH and salt concentration on the binding of BV to smURFP was investigated. Aliquots of the smURFP proteins were added to a 50 mM Tris-HCl buffer solution at different pH (7.4, 8, 9.4, and 11) to a final concentration of 1 μM. Also, BV solutions were prepared at different pH to a final concentration of 10 μM. Meanwhile, solutions of smURFP and BV were prepared in 50 mM Tris-HCl, pH 8 buffer solution at different salt concentrations (over the range of 0 mM−1000 mM NaCl). Fluorescence of smURFP + BV was measured at the above different buffer conditions. The dissociation

constant between BV and smURFP in different buffer conditions were then carried out at 4 °C with the GE Microcal iTC 200, using 250 rpm stirring and 90 s delay between succeeding injections to the sample cell (800 μL). The first injection of a reduced volume (0.2 μL) of BV sample was followed by 18 injections of 2 μL. The sample cell was filled with smURFP solution (100 μM) while 50 mM BV solution was placed in the syringe. The solubility of the BV chromophore in different buffer conditions was also measured by the Thermo Fisher Scientific UV–Vis Nano Drop 2000 spectrophotometer. All samples were assayed in duplicate.

2.5. Characterization of the BV detection sensor

BV solutions were prepared in optimal buffer, buffer 1 (50 mM Tris-HCl, pH 7.4, 900 mM NaCl) and buffer 2 (50 mM Tris-HCl, pH 8, 0 mM NaCl), respectively, to a series of different final concentrations (0.5, 1, 2.5, 5, 10, 15, 20, 25, 30, 40, and 50 μM). smURFP solution was prepared to a final concentration of 100 μM in optimal buffer, buffer 1 and buffer 2, respectively. Samples were mixed and fluorescence was measured after incubation. All samples were assayed in duplicate. Calibration standards ranging from 0.001 μM to 25 μM were added to the plate for each measurement. Linear regression was used to calculate the equation for determining of BV concentration. The limit of detection (LOD) was determined by calculation from the yield of fluorescence of the negative control, increased by 3× standard deviation (SD): $LOD = mean_{blank} + 3 \times SD$. The limit of detection (LOD) was determined by calculation from the yield of fluorescence of the negative control, increased by 3× standard deviation (SD): $LOQ = mean_{blank} + 10 \times SD$.

2.6. Sensing of BV in serum

Biological BV samples were prepared by spiking human serum and chicken serum with known concentration of BV solution to give various concentrations (1, 5, 10, 25, 50, 100, 500, 1000, 5000, and 10,000 μM). Standard BV samples were prepared in optimal buffer to different concentrations as well. smURFP solution was prepared in the optimal buffer to a concentration of 100 μM. Biological BV samples whose concentration was higher than 25 μM were diluted to 10 μM in optimal buffer. Fluorescence was measured after incubation. Each sample was assayed in duplicate, and the concentration was compared with the actual concentration by calculating the relative error. In addition, solutions containing single or combination of molecules (BV only, BR only, hematin only, $BVMe_2$ only, BV + BR, BV + hematin, BV + $BVMe_2$, and BV + BR + hematin + $BVMe_2$) were prepared in the same procedure to determine the selectivity of BV assays.

2.7. Pretreatment of clinical samples

Clinical BV samples were prepared by diluting real human serum sample to 40% in optimal buffer. Centrifuge the diluted sample for at 4 °C, 15,000×*g* for 30 min. 50 μL of diluted sample was placed into black 96-well plates, followed by 50 μL of 100 μM purified smURFP in optimal buffer. Fluorescence was measured after incubation. 50 μL of diluted samples were further diluted by spiking with 50 μL optimal buffer and 100 μL of 20% clinical serum samples were used for LC-MS method. Patient's serum samples were provided by Tianjin Women's and Children's Health Centre (TWCHC) and the above substances were used as provided.

2.8. LC-MS analysis of BV

The quantitative analysis of BV by LC-MS was perfomed using Triple Quad Mass Spectrometer (Agilent, USA) and operated in the positive ion mode. Each sample (20 μL) was injected into a 250 × 4.6 mm HyPURITY™ C18 column (Thermo Scientific, USA) with a flow rate of 0.8 mL/min. For gradient elution, mobile phase A was H_2O/acetonitrile/HCOOH = 98/2/0.1 and mobile phase B was H_2O/acetonitrile/HCOOH = 2/98/0.1. The linear and stepwise gradient was programmed as follows: 0–1 min: 10% solvent B; 1–1.5 min: 10–49% solvent B; 1.5–3 min: 49% solvent B; 3–13 min: 49–52% solvent B; 13–13.5 min: 52–100% solvent B; 13.5–14 min: 100-10% solvent B; 14–20 min: 10% solvent B. BV was detected in MRM mode by monitoring the transitions of the *m/z* 583 to 297. The spray voltage was 3500 V, the vaporizer temperature was 275 °C, and the ion transfer tube temperature was 350 °C. Calibration curve was determined using standard BV samples which were prepared by spiking human serum with known concentration of BV solution to give various concentrations (0.00001, 0.0001, 0.001, 0.01, 0.1, 10, and 25 μM). When determining calibration curve using HPLC mode, BV was detected in DAD mode by monitoring the absorbance at 388 nm.

3. Results and discussion

3.1. Purification and characterization of smURFP

Rodriguez et al. found that the smURFP + BV complex initially formed a nonfluorescent high-affinity complex before covalent attachment to BV [25]. This result indicated that the development of fluorescence by smURFP + BV involved two-step kinetics, which comprised of non-covalent BV binding and covalent BV attachment as shown in Fig. 1A. Fig. 1B shows that smURFP can covalently bind BV through the C52 residue [26], which is the basis for us to develop a BV detection sensor. The non-covalent binding of BV to smURFP was elucidated by the recently reported 3D structure of smURFP + BV [26]. Amino acids such as R47, R54, D55, S77, I78, S89, and S100 interacted with BV through hydrogen bonding in the binding pocket of BV except for the C52 residue that covalently interacted with BV (Fig. 1B). This high-resolution structure confirmed that non-covalent bonds also contributed to the binding of BV to smURFP. It is known that the non-covalent interactions between molecules are controlled by several forces such as hydrogen bonds, electrostatic interactions, hydrophobic, and van der Waals forces [27,28]. Among them, hydrophobic and electrostatic forces are much stronger than hydrogen bonding and van der Waals forces [29,30]. Fig. 1C and D shows the charge distribution and degrees of hydrophobicity of the binding pocket of smURFP, respectively. Fig. 1C shows that the empty BV binding pocket of smURFP was surrounded by positive charges. In contrast, there were marked changes in the electrostatic surface potential map of this binding pocket after BV binding as no obvious changes shown in hydrophobicity map between before and after the binding of BV (Fig. 1D). All these structural features strongly implied that non-covalent interaction such as electrostatic force may be involved in the binding of BV to smURFP. Therefore, we proposed that we could enhance the binding of BV to smURFP by intentionally optimizing the physical non-covalent interactions between them to increase the final fluorescence of smURFP and ultimately to increase the sensitivity of our sensor.

To test our idea, we firstly produce the smURFP protein that was intended to be used as the BV-sensing element. Fig. 1E shows the result of purification of smURFP with gel filtration chromatography suggested high purity of smURFP after purification. According to the previous reports, only BV bound to the active smURFP could produce fluorescence [25,31]. As shown in Fig. 1F, fluorescence was generated only when the smURFP was mixed with BV as neither the protein itself nor the BV could individually produce fluorescent signals. These results indicated that smURFP maintained biological

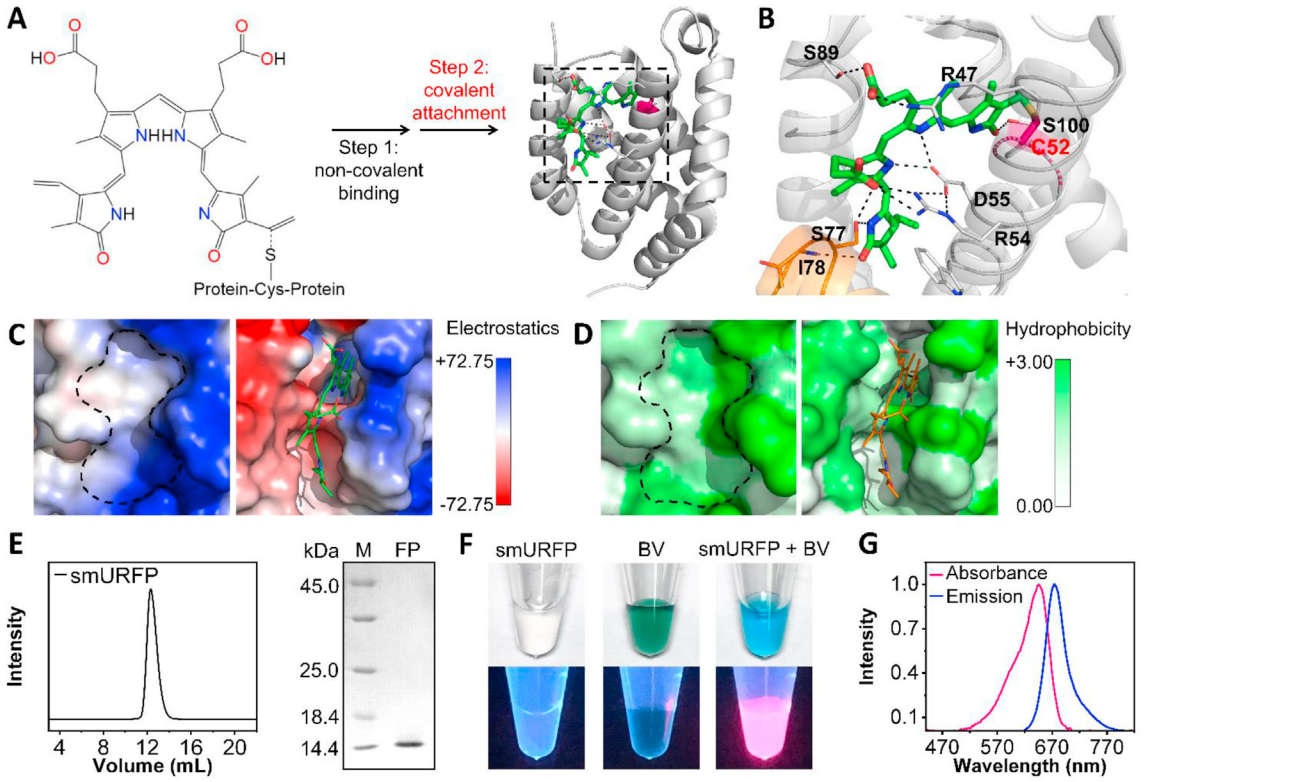

Fig. 1. Purification and characterization of smURFP. (A) Two-step binding between BV and smURFP. **(B)** X-ray crystal structure of smURFP covalently bound to BV through the C52 residue and interaction of amino acids with BV through hydrogen bonding in the BV-binding pocket (PDB 6FZN). **(C–D)** The charge distribution and hydrophobicity degrees of the BV-binding pocket (PDB 6FZO; PDB 6FZN). The left is pocket without a BV chromophore and the right is pocket with a covalently bound BV chromophore. **(E)** Gel filtration chromatography and SDS-PAGE of smURFP **(F)** Comparison of smURFP, BV, and smURFP + BV. The top indicates white light and the bottom indicates fluorescence. **(G)** Normalized absorbance and fluorescence spectra of smURFP with different concentrations of BV.

activity after the production process. The absorbance and emission spectra of smURFP + BV were also characterized using different concentrations of BV (Fig. 1G and Fig. S1A&B). A peak at 642 nm was the characteristic absorbance peak of the complex of smURFP + BV. The characteristic peaks at about 390 nm and 280 nm were attributed to the absorbance signals of BV (Fig. S1C) and smURFP protein (Fig. S1D) respectively. The emission spectra of smURFP contained a major peak centered at 670 nm, which was consistent with the previous report [25]. It was evident that the BV concentration had a marked effect on the intensity of fluorescence emission of smURFP + BV. This result strengthened our hypothesis that BV concentration can be measured by monitoring the changes in the emission intensity of smURFP + BV.

3.2. Optimization of the binding of BV to smURFP

After we obtained the purified smURFP, we developed the sensor by first optimizing the non-covalent binding conditions of BV to smURFP based on our hypothesis. It is well known that several physical parameters including pH and salt concertation can influence the non-covalent interaction between molecules [32–34]. Hence, we systematically investigated the effects of pH and salt concertation on the binding of BV to smURFP. As we mentioned above, the fluorescence of smURFP was dependent on the binding of BV to smURFP. Therefore, we measured the fluorescence of smURFP + BV complex at different pH values and salt concentrations to optimize their interaction. As shown in Fig. 2A, pH had a visible influence to the binding of BV to smURFP. The complex showed the highest fluorescence intensity at pH 8. When the pH values were lower or higher than 8, the fluorescence intensities of the smURFP + BV complex were decreased. The salt concentration also affected the outcome of the fluorescence of the smURFP + BV complex (Fig. 2A). The fluorescence of the complex increased rapidly with the increase of salt concentration, and gradually reached a plateau at the concentration of 900 mM NaCl. Moreover, we measured the K_d between BV and smURFP in the same conditions as mentioned above to further optimize the physical conditions for the binding of BV to smURFP. As shown in Fig. 2B, it was evident that pH affected the K_d between BV and smURFP. The lowest K_d value was obtained at pH 8 reflecting a strong interaction between BV and smURFP at this condition. Fig. 2B shows that the concentration of NaCl also had an obvious impact on the K_d values of the smURFP + BV complex with the lowest K_d attained at 900 mM NaCl. At this stage, we conclude that physical conditions influence the binding of BV to smURFP. The optimal pH and salt concentration we obtained for further sensor construction was found to be pH 8 and 900 mM NaCl. Besides, considering pH and salt concentration affected the outcome of the fluorescence of smURFP + BV complex, we inferred that this may be due to the changes in the binding amount of BV to the smURFP resulting in different fluorescence intensities. We, therefore, measured the relative chromophorylation by comparing the typical absorption of BV (388 nm) with protein absorption at 280 nm, providing an indication of the amount of bound BV to smURFP at the above-mentioned conditions. As shown in Fig. 2C, the pattern of change in the binding amount of BV to smURFP was identical to the fluorescence intensities of the smURFP + BV complex at different pH and salt conditions. These optimization results indicated that physical conditions directly influenced the binding amount of BV to smURFP.

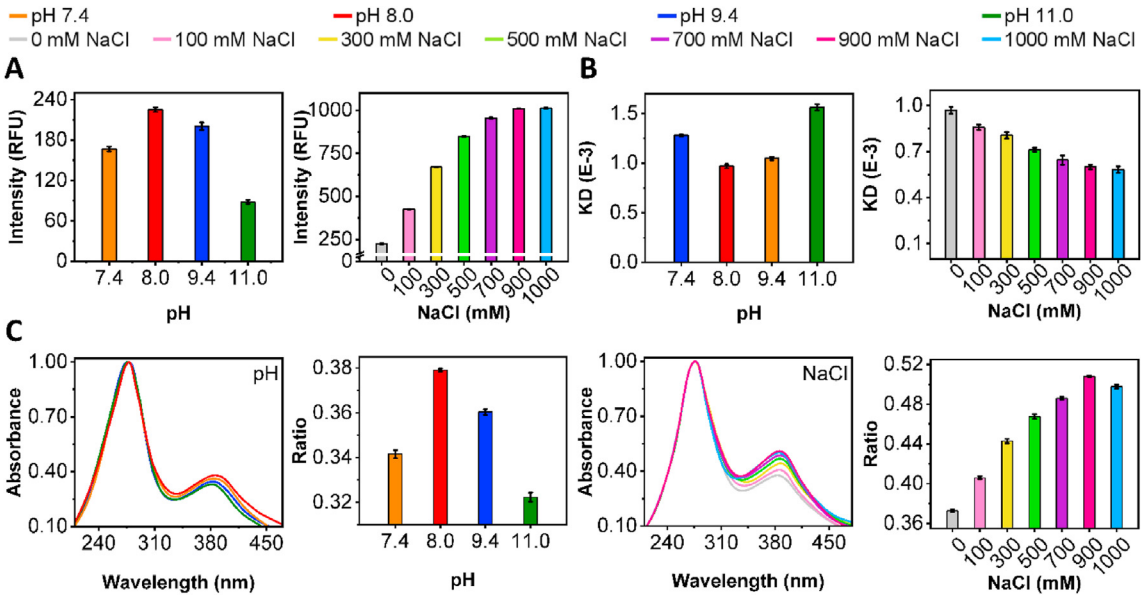

Fig. 2. Optimization of the condition for smURFP + BV. (A) Fluorescence intensity of the binding of BV to smURFP at different pH and NaCl concentrations. **(B)** The dissociation constant of the smURFP + BV complex at different pH and NaCl concentrations. **(C)** Binding amount of BV to smURFP at different pH values and salt concentrations.

3.3. Characterization of BV detection sensor

As shown in Fig. 3A, the fluorescence of the smURFP + BV complex increased rapidly with an increase in BV concentration and gradually reached a plateau after the concentration of BV reached 25 μM. Therefore, the linear range of our sensor was determined within the range of 0 μM–25 μM of BV at the optimal buffer condition. Also, the linearity is well demonstrated in human serum solution (Fig. 3B) and chicken serum solution (Fig. 3C). In healthy individuals, BV levels are low in the plasma and are strongly correlated with BR as BVR can efficiently reduce BV to BR in the peripheral organs [9,35]. Moreover, it has been reported that a low concentration of BV had a direct influence on the inflammatory and antiviral response *in vivo* [3,36]. These published data indicated that the linear range of our sensor was suitable for biological and medical studies. Fig. 3D shows that the LOD of our sensor was 0.4 nM in the buffer solution. To the best of our knowledge, this is the lowest LOD that has ever been reported. We also determined the LOD of our sensor in human (Fig. 3E) and chicken serum (Fig. 3F) and the results showed that the LOD remained as low as

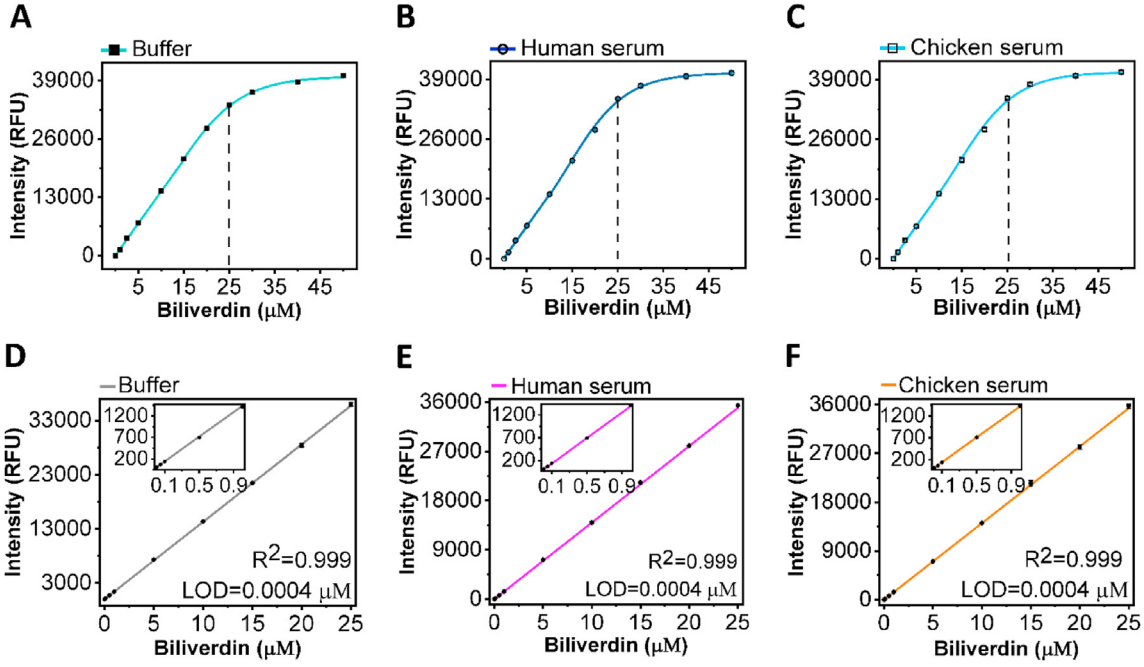

Fig. 3. Determination of the linear range and calibration curve. (A) Fluorescence intensity of smURFP + BV over the BV concentration range of 0 μM–50 μM in optimal buffer condition, **(B)** human serum solution, and **(C)** chicken serum solution. **(D)** Calibration curve in the linear range of 0 μM–25 μM BV in the optimal buffer condition, **(E)** human serum solution, and **(F)** chicken serum solution.

Table 1
Summary of the published reports of determining BV concentration.

BV sample	Method	Detection limit (nM)	Linear range (μM)	Reference
Chicken/human serum	smURFP	0.4	0–25	This work
Chicken serum	iRFP	20	0–10	[37]
Avian liver and spleen	iRFP	3.1	0–1	[38]
Human serum	HPLC-TLS/HPLC-DAD	1.2/60	0.0025–0.25/0.01–0.5	[19]
PBS	FERS	130	0–2.5	[22]
Pericardial fluid	HPLC	310	0–8.3	[39]
Water medium	L-cys-CuNCs	233	0.5–40	[23]

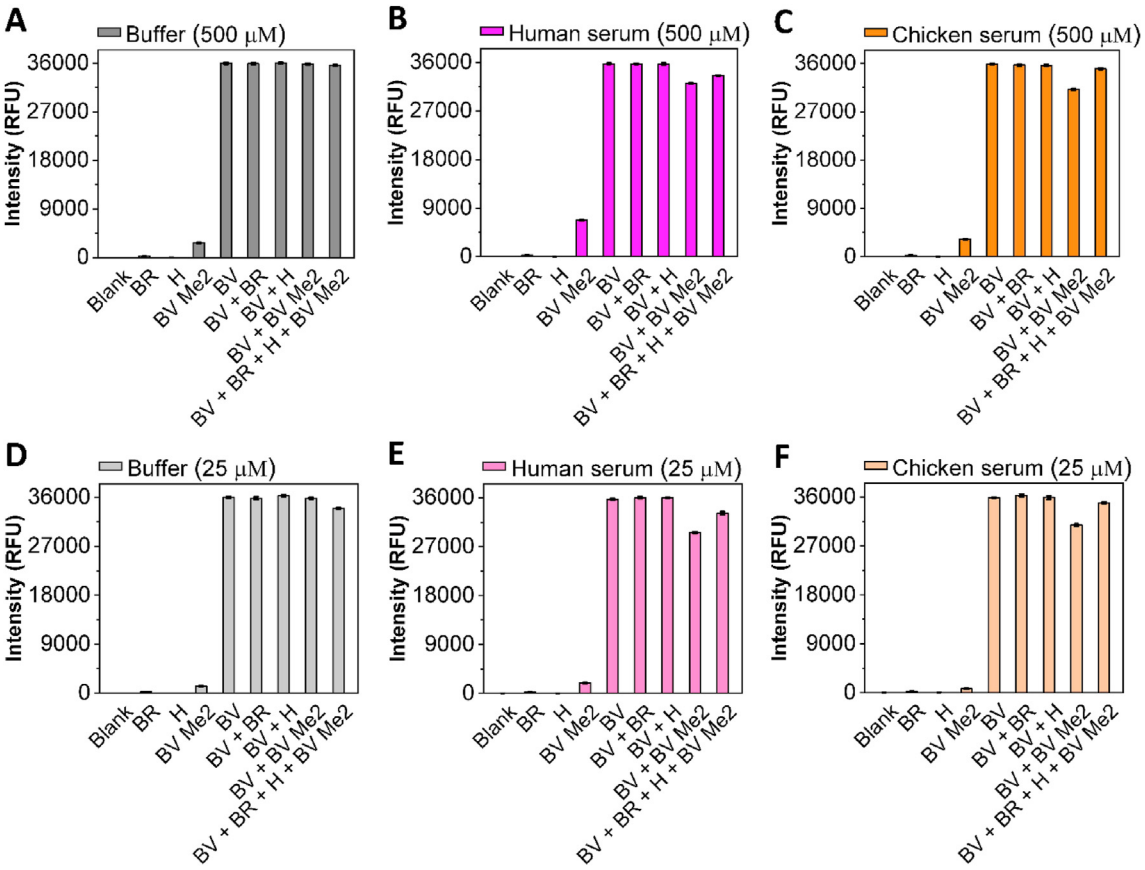

Fig. 4. Determination of the selectivity of smURFP. (A) Fluorescence intensity of smURFP after addition of 25 μM BV, 500 μM BR, 500 μM hematin, and 500 μM $BVMe_2$ in optimal buffer condition, **(B)** human serum solution, and **(C)** chicken serum solution. **(D)** Fluorescence intensity of smURFP after addition of 25 μM BV, 25 μM BR, 25 μM hematin, and 25 μM $BVMe_2$ in optimal buffer condition, **(E)** human serum solution, and **(F)** chicken serum solution. The optimal buffer condition was pH 8 and 900 mM NaCl. Blank: sample without molecules. H: hematin.

0.4 nM in these conditions. The comparisons of our LOD and linear range with other studies have been summarized in Table 1. Meanwhile, the LOQ and sensitivity in buffer and serum solution were determined to be 1.4 nM and 16.0 RFU[1] nM^{-1} in buffer, 1.5 nM and 11.7 RFU nM^{-1} in human serum, and 1.2 nM and 10.9 RFU nM^{-1} in chicken serum, respectively. All calibration curves used for determining BV concentrations had R^2 values greater than 0.999. To prove that our optimization did cause positive influences on the linear range of the calibration curve and the sensitivity of the sensor, as well. We determined the linear range and calibration curves in conditions that are not the optimal one. Any change in the pH (Fig. S3A) or salt concentration (Fig. S3B) decreased the linear range of our sensor indicating that the physical conditions significantly influence the linear range as well.

BR and hematin are two of the most common BV analogs in mammalian blood as both these molecules contain a tetrapyrrolic structure, which may cause a non-specific binding to the smURFP. Therefore, competitive recognition studies were also carried out in presence of those two interfering molecules at low (25 μM) and high concentrations (500 μM) in buffer, human serum and chicken serum (Fig. 4). Our sensor selectively sensed BV irrespective of the concentration or combination of the BR and hematin. Together, this data indicated that our sensor was able to detect BV specifically in serum.

3.4. Sensing of BV in serum

As the major challenge for BV detection is its quantification in a complex biological fluid-like serum, we applied our sensor to

[1] RFU: Relative fluorescence units.

Table 2
Accuracy of determination of BV concentration in serum.[a]

Actual concentration (μM)	Determined concentration (μM)	Relative error
Human serum		
0	< LOD	ND
1	1.01 ± 0.05	0.05
5	5.14 ± 0.22	0.04
10	10.05 ± 0.60	0.06
25	25.24 ± 0.69	0.03
50	49.95 ± 1.04	0.02
100	100.26 ± 2.41	0.02
500	500.54 ± 5.49	0.01
1000	1005.72 ± 18.31	0.02
5000	4999.31 ± 122.33	0.02
10,000	10038.43 ± 291.49	0.03
Chicken serum		
0	< LOD	ND
1	1.01 ± 0.04	0.03
5	5.00 ± 0.21	0.04
10	10.01 ± 0.42	0.04
25	25.27 ± 0.84	0.03
50	50.08 ± 0.76	0.01
100	100.08 ± 1.03	0.01
500	501.48 ± 15.45	0.03
1000	998.75 ± 25.05	0.02
5000	5017.66 ± 63.81	0.02
10,000	9995.92 ± 207.42	0.02

[a] Each sample was assayed in duplicate. < LOD = below the limit of detection; ND = not determined.

detect different amounts of BV in human and chicken serum samples. Briefly, certain known concentrations of BV were added into healthy chicken and human serum. The reliability of our senor was verified by comparing the measured concentrations of BV by our sensor with the pre-determined concentrations of the added BV. The results obtained confirmed the reliability of our biosensor system in quantitative BV detection in both human and chicken serum (Table 2), and buffer (Table S1) as well.

3.5. Quantification analysis of BV in clinical samples and comparison with LC-MS method

The clinical human serum samples were collected from 25 different human blood, of which sample No. #1-1 to #1–5 were from BR test negative patients, and sample No. #2-1 to 3–12 were from BR test half-positive or positive patients who were suspected to have hepatic disease. Clinical BV samples were quantitatively analyzed both using our biosensor system, traditional LC-MS method, and HPLC method as well to verify the reliability of our senor by comparing those three different methods. The LOD of LC-MS and HPLC method is 0.006 μM (Fig. S5) and 0.02 μM (Fig. S6), respectively, which is higher than our sensor. The results obtained confirmed the reliability of both our biosensor system in quantitative BV detection and traditional LC-MS method in real clinical human serum sample (Table 3). It shows generally higher BV concentrations in samples from suspected hepatic disease patients in both quantitative analysis results. It shows some differences between the two numerical value when the BV concentration calculated to be relatively low as there is no huge difference when the BV concentration was higher. However, it shows that our sensor does have enough sensitivity in determining BV concentration in real samples.

4. Conclusions

We systematically exploited and optimized the physical interaction between BV and a far-infrared fluorescent protein smURFP to increase the sensitivity of a BV detection biosensor. Structure based optimization strategy used in our study can be applied to other similar studies to increase biosensor sensitivity. Our sensing system has a high potential for quantification of large numbers of samples in clinical research. In addition, other BV-related detection is also very easy to be implemented based on our current system. For example, we can convert BV to BV to detect its concentration.

Table 3
Quantitative determination of BV concentration in clinical sample.[a]

Clinical sample	smURFP		LC-MS	
	Determined concentration (μM)	Relative error	Determined concentration (μM)	Relative error
#1-1	0.37 ± 0.14	0.03	0.42 ± 0.03	0.02
#1-2	0.49 ± 0.24	0.03	0.60 ± 0.04	0.03
#1-3	0.65 ± 0.24	0.03	0.65 ± 0.03	0.02
#1-4	0.48 ± 0.16	0.02	0.26 ± 0.04	0.03
#1-5	0.44 ± 0.06	0.06	0.32 ± 0.03	0.02
#2-1	0.51 ± 0.09	0.02	0.49 ± 0.04	0.03
#2-2	0.35 ± 0.10	0.02	0.35 ± 0.09	0.04
#2-3	0.91 ± 0.12	0.03	0.94 ± 0.03	0.02
#2-4	0.95 ± 0.09	0.02	0.94 ± 0.03	0.02
#2-5	0.51 ± 0.14	0.03	0.55 ± 0.03	0.02
#2-6	0.56 ± 0.09	0.03	0.24 ± 0.03	0.02
#2-7	0.47 ± 0.13	0.02	0.25 ± 0.06	0.02
#2-8	0.98 ± 0.09	0.02	0.97 ± 0.07	0.03
#3-1	1.53 ± 0.10	0.02	1.13 ± 0.06	0.04
#3-2	0.97 ± 0.18	0.04	1.00 ± 0.04	0.03
#3-3	0.89 ± 0.06	0.01	0.84 ± 0.04	0.03
#3-4	0.98 ± 0.03	0.04	0.98 ± 0.05	0.03
#3-5	1.34 ± 0.09	0.03	1.27 ± 0.03	0.03
#3-6	0.91 ± 0.17	0.04	0.80 ± 0.07	0.02
#3-7	1.86 ± 0.14	0.03	1.88 ± 0.07	0.04
#3-8	1.92 ± 0.16	0.02	1.91 ± 0.10	0.04
#3-9	2.69 ± 0.19	0.02	2.72 ± 0.08	0.04
#3-10	2.71 ± 0.17	0.02	2.50 ± 0.08	0.04
#3-11	2.25 ± 0.31	0.03	2.24 ± 0.07	0.04
#3-12	2.19 ± 0.02	0.02	2.19 ± 0.08	0.04

[a] Each sample was assayed in duplicate.

The proposed method has a high applicability as commercial kits or protocol as the use of the biophysically the brightest near-infrared fluorescent protein smURFP which covalently bind to BV makes the limit of detection of the method the lowest that has ever been reported for a BV biosensor to our knowledge. But the methods also have some limits that it still needs further optimization and development to decrease the detection error in relatively low BV concentration range, so that it could have greater applicability of clinical use.

Author contribution

Xiaqing Zhu: Methodology, Investigation, Data Curation, Writing-Original Draft. Shuren Feng: Collecting patient's serum samples, Investigation. Zhongyi Jiang: Investigation. Huayue Zhang: Investigation. Yanyan Wang: Writing-Review & Editing, Resources. Haitao Yang: Conceptualization. Zefang Wang: Conceptualization, Project administration, Writing-Review & Editing Resources.

Declaration of competing interest

The authors declare that they have no known competing financial interests or personal relationships that could have appeared to influence the work reported in this paper.

Acknowledgements

This work was supported by the National Natural Science Foundation of China acknowledged by Zefang Wang [grant numbers 31970048, 81601593]; the National Natural Science of China acknowledged by Yanyan Wang [grant number 61971302].

Appendix A. Supplementary data

Supplementary data to this article can be found online at https://doi.org/10.1016/j.aca.2021.338709.

References

[1] W. Osiak, S. Wątroba, L. Kapka-Skrzypczak, J. Kurzepa, Two faces of heme catabolic pathway in newborns: a potential role of bilirubin and carbon monoxide in neonatal inflammatory diseases, Oxid. Med. Cell. Longev. 2020 (2020) 7140496.
[2] L.E. Otterbein, R. Foresti, R. Motterlini, Heme oxygenase-1 and carbon monoxide in the heart, Circ. Res. 118 (12) (2016) 1940–1959.
[3] A. Zhang, B. Wan, D. Jiang, Y. Wu, P. Ji, Y. Du, G. Zhang, The cytoprotective enzyme heme oxygenase-1 suppresses pseudorabies virus replication *in vitro*, Front. Microbiol. 11 (2020) 412.
[4] B. Wu, Y. Wu, W. Tang, Heme catabolic pathway in inflammation and immune disorders, Front. Physiol. 10 (2019) 825.
[5] H.M. Schipper, W. Song, A. Tavitian, M. Cressatti, The sinister face of heme oxygenase-1 in brain aging and disease, Prog. Neurobiol. 172 (2019) 40–70.
[6] M. Nitti, A.L. Furfaro, G.E. Mann, Heme oxygenase dependent bilirubin generation in vascular cells: a role in preventing endothelial dysfunction in local tissue microenvironment? Front. Physiol. 11 (2020) 23.
[7] Z. Wang, Q. Qi, Gut microbial metabolites associated with HIV infection, Future Virol. 14 (5) (2019) 335–347.
[8] K. Hu, Z. Zhu, M.M. Mathahs, H. Tran, J. Bommer, C.A. Testa, W.N. Schmidt, Metalloprotoporphyrin inhibition of HCV NS3-4A protease: structure-activity relationships, Drug Des. Dev. Ther. 14 (2020) 757–771.
[9] B. Wegiel, L.E. Otterbein, Go green: the anti-inflammatory effects of biliverdin reductase, Front. Pharmacol. 3 (2012) 47.
[10] B. Bakrania, E.F. Du Toit, K.-H. Wagner, J.P. Headrick, A.C. Bulmer, Pre- or post-ischemic bilirubin ditaurate treatment reduces oxidative tissue damage and improves cardiac function, Int. J. Cardiol. 202 (2016) 27–33.
[11] P. Fathi, H.J. Knox, D. Sar, I. Tripathi, F. Ostadhossein, S.K. Misra, M.B. Esch, J. Chan, D. Pan, Biodegradable biliverdin nanoparticles for efficient photoacoustic imaging, ACS Nano 13 (7) (2019) 7690–7704.
[12] R. Xing, Q. Zou, C. Yuan, L. Zhao, R. Chang, X. Yan, Self-assembling endogenous biliverdin as a versatile near-infrared photothermal nanoagent for cancer theranostics, Adv. Mater. 31 (16) (2019), a1900822.
[13] R. van Dijk, S.J. Aronson, D.R. de Waart, S.F. van de Graaf, S. Duijst, J. Seppen, R.O. Elferink, U. Beuers, P.J. Bosma, Biliverdin reductase inhibitors did not improve severe unconjugated hyperbilirubinemia *in vivo*, Sci. Rep. 7 (1) (2017) 1646.
[14] I. Galván, P.R. Camarero, R. Mateo, J.J. Negro, Porphyrins produce uniquely ephemeral animal colouration: a possible signal of virginity, Sci. Rep. 6 (1) (2016) 39210.
[15] H. Ahyayauch, A.B. García-Arribas, J. Sot, E.J. González-Ramírez, J.V. Busto, B.G. Monasterio, N. Jiménez-Rojo, F.X. Contreras, A. Rendón-Ramírez, C. Martin, A. Alonso, F.M. Goñi, Pb(II) induces scramblase activation and ceramide-domain generation in red blood cells, Sci. Rep. 8 (1) (2018) 7456.
[16] H.Y.A. Darwish, S.B. Dalirsefat, X. Dong, G. Hua, J. Chen, Y. Zhang, J. Li, J. Xu, J. Li, X. Deng, C. Wu, Genome-wide association study and a post replication analysis revealed a promising genomic region and candidate genes for chicken eggshell blueness, PloS One 14 (1) (2019), e0209181.
[17] D.-P. Bai, X.-Y. Lin, Y. Wu, S.-Y. Zhou, Z.-b. Huang, Y.-F. Huang, A. Li, X.-H. Huang, Isolation of blue-green eggshell pigmentation-related genes from Putian duck through RNA-seq, BMC Genom. 20 (1) (2019) 66.
[18] S.T. Williams, S. Ito, K. Wakamatsu, T. Goral, N.P. Edwards, R.A. Wogelius, T. Henkel, L.F.C. de Oliveira, L.F. Maia, S. Strekopytov, T. Jeffries, D.I. Spe spespeiser, J.T. Marsden, Identification of shell colour pigments in marine snails clanculus pharaonius and C. margaritarius (Trochoidea; Gastropoda), PloS One 11 (7) (2016), e0156664.
[19] M. Martelanc, L. Žiberna, S. Passamonti, M. Franko, Application of high-performance liquid chromatography combined with ultra-sensitive thermal lens spectrometric detection for simultaneous biliverdin and bilirubin assessment at trace levels in human serum, Talanta 154 (2016) 92–98.
[20] N.S. Nytofte, M.A. Serrano, M.J. Monte, E. Gonzalez-Sanchez, Z. Tumer, K. Ladefoged, O. Briz, J.J.G. Marin, A homozygous nonsense mutation (c.214C→A) in the biliverdin reductase alpha gene (BLVRA) results in accumulation of biliverdin during episodes of cholestasis, J. Med. Genet. 48 (4) (2011) 219–225.
[21] S. Iwamori, E. Sato, D. Saigusa, K. Yoshinari, S. Ito, H. Sato, N. Takahashi, A novel and sensitive assay for heme oxygenase activity, Am. J. Physiol. Ren. Physiol. 309 (7) (2015) F667–F671.
[22] D. Yan, C. Domes, R. Domes, T. Frosch, J. Popp, M.W. Pletz, T. Frosch, Fiber enhanced Raman spectroscopic analysis as a novel method for diagnosis and monitoring of diseases related to hyperbilirubinemia and hyperbiliverdinemia, Analyst 141 (21) (2016) 6104–6115.
[23] S.K. Anand, M.R. Mathew, K.G. Kumar, A simple and cost effective turn off fluorescence sensor for biliverdin and bilirubin based on L-cysteine modulated copper nanoclusters, J. Fluoresc. 30 (1) (2020) 63–70.
[24] P. Novotná, F. Králík, M. Urbanová, Chiral recognition of bilirubin and biliverdin in liposomes and micelles, Biophys. Chem. 205 (2015) 41–50.
[25] E.A. Rodriguez, G.N. Tran, L.A. Gross, J.L. Crisp, X. Shu, J.Y. Lin, R.Y. Tsien, A far-red fluorescent protein evolved from a cyanobacterial phycobiliprotein, Nat. Methods 13 (9) (2016) 763–769.
[26] J.P. Fuenzalida-Werner, R. Janowski, K. Mishra, I. Weidenfeld, D. Niessing, V. Ntziachristos, A.C. Stiel, Crystal structure of a biliverdin-bound phycobiliprotein: interdependence of oligomerization and chromophorylation, J. Struct. Biol. 204 (3) (2018) 519–522.
[27] D. Kagra, P.S. Prabhakar, K.D. Sharma, P. Sharma, Structural patterns and stabilities of hydrogen-bonded pairs involving ribonucleotide bases and arginine, glutamic acid, or glutamine residues of proteins from quantum mechanical calculations, ACS Omega 5 (7) (2020) 3612–3623.
[28] M. Samperi, L. Pérez-García, D.B. Amabilino, Quantification of energy of activation to supramolecular nanofibre formation reveals enthalpic and entropic effects and morphological consequence, Chem. Sci. 10 (44) (2019) 10256–10266.
[29] S. Singh, A. Nazabal, S. Kaniyappan, J.-L. Pellequer, A.S. Wolberg, D. Imhof, J. Oldenburg, A. Biswas, The plasma factor XIII heterotetrameric complex structure: unexpected unequal pairing within a symmetric complex, Biomolecules 9 (12) (2019) 765.
[30] W. Zierkiewicz, M. Michalczyk, S. Scheiner, Competition between intra and intermolecular triel bonds. complexes between naphthalene derivatives and neutral or anionic Lewis bases, Molecules 25 (3) (2020) 635.
[31] A.A. Shemetov, O.S. Oliinyk, V.V. Verkhusha, How to increase brightness of near-infrared fluorescent proteins in mammalian cells, Cell Chem. Biol. 24 (6) (2017) 758–766, e3.
[32] M. Majewski, S. Ruiz-Carmona, X. Barril, An investigation of structural stability in protein-ligand complexes reveals the balance between order and disorder, Commun. Chem. 2 (1) (2019) 110.
[33] S.E. Boyken, M.A. Benhaim, F. Busch, M. Jia, M.J. Bick, H. Choi, J.C. Klima, Z. Chen, C. Walkey, A. Mileant, A. Sahasrabuddhe, K.Y. Wei, E.A. Hodge, S. Byron, A. Quijano-Rubio, B. Sankaran, N.P. King, J. Lippincott-Schwartz, V.H. Wysocki, K.K. Lee, D. Baker, De novo design of tunable, pH-driven conformational changes, Science 364 (6441) (2019) 658–664.
[34] C.P. Papaneophytou, A.I. Grigoroudis, C. McInnes, G. Kontopidis, Quantification of the effects of ionic strength, viscosity, and hydrophobicity on protein–ligand binding affinity, ACS Med. Chem. Lett. 5 (8) (2014) 931–936.
[35] J. Nam, Y. Lee, Y. Yang, S. Jeong, W. Kim, J.-W. Yoo, J.-O. Moon, C. Lee, H.Y. Chung, M.-S. Kim, S. Jon, Y. Jung, Is it worth expending energy to convert biliverdin into bilirubin? Free Radic. Biol. Med. 124 (2018) 232–240.
[36] G. Canesin, S.M. Hejazi, K.D. Swanson, B. Wegiel, Heme-derived metabolic signals dictate immune responses, Front. Immunol. 11 (2020) 66.

[37] A. Berlec, B. Štrukelj, A high-throughput biliverdin assay using infrared fluorescence, J. Vet. Diagn. Invest. 26 (4) (2014) 521–526.
[38] M.W. Butler, S.C. Bociulis, A.R. Little, J.A. Minnick, N.J. Ritter, M.E. Rockman, M.L. Rossi, J.K. Hines, Quantifying biliverdin in liver and spleen samples from multiple avian species, Auk 134 (2016) 11–21.
[39] M. Mizobe, F. Kondo, K. Kumamoto, Y. Kanda, H. Seguchi, High-performance liquid chromatographic analysis of bilirubin and biliverdin from jaundiced broilers, J. Vet. Med. Sci. 59 (8) (1997) 677–680.